Biochemistry and Biophysics Reports 29 (2022) 101188

Contents lists available at ScienceDirect

Biochemistry and Biophysics Reports

journal homepage: www.elsevier.com/locate/bbrep

Utilizing *in silico* and *in vitro* methods to identify possible binding sites of a novel ligand against *Pseudomonas aeruginosa* phospholipase toxin ExoU

Krista Chamberlain [a], Mya Johnson [b], Terry-Elinor Reid [a], Tzvia I. Springer [a,*]

[a] Pharmaceutical Sciences Department, School of Pharmacy, Concordia University Wisconsin, Mequon, WI, 53097, USA
[b] Harvard Faculty of Arts and Science, School of Engineering and Applied Sciences, 150 Western Ave, Boston, MA, 02134, USA

ARTICLE INFO

Keywords:
Phospholipase
ExoU
Saturation transfer nuclear magnetic resonance
Pseudomonas aeruginosa

ABSTRACT

Multi-drug resistant infections caused by the opportunistic pathogen, *Pseudomonas aeruginosa (P. aeruginosa),* are a continuing problem that contribute to morbidity and mortality in immunocompromised hosts such as cystic fibrosis (CF), wound and burn patients. The bacterial toxin ExoU is one of four potent toxins that *P. aeruginosa* secretes into the epithelial cells of hosts. In this study, NMR Saturation Transfer Difference (STD) and *in silico* Schrödinger Computational Modeling were used to identify a possible binding site of a novel ligand methoctramine targeting ExoU. Future project goals will be to design a structure activity relationship (SAR) study of methoctramine and ExoU and lead to a new drug solving ExoU toxicity *P. aeruginosa* exerts in the clinical environment.

1. Introduction

Pseudomonas aeruginosa (P. aeruginosa) is an opportunistic multidrug-resistant pathogen that commonly infects cystic fibrosis, burn and wound patients [1–3]. *P. aeruginosa* secretes via a type III secretion system (T3SS) various effector proteins (ExoS, ExoT, ExoY, ExoU) inside mammalian host cells; ExoU, is a phospholipase A2 (PLA2) enzyme activated by host ubiquitin (Ub) and ubiquitinated proteins [4–9]. When activated, ExoU exerts membrane destructive activity leading to host cell death [6,7]. Although there are current treatments and studies identifying polyamines and other antibiotics against *P. aeruginosa*, there is currently no drug on the market targeting ExoU [2,10]. The only current known inhibitor for ExoU includes methyl arachidonoyl fluorophosphate (MAFP), an irreversible and non-selective phospholipase inhibitor, which is detrimental to all variations of phospholipids. Because the aim is to discover a 'drug-like' ligand small molecule, MAFP was not considered in this research as it does not match the criteria. The current X-ray crystallographic structure of ExoU (74 kDa) is incomplete and lacks a mechanism of activation between ExoU, Ub, and the phospholipid membrane [11]. However, the availability of ExoU-SpcU complex 1.92Å X-ray structure [12] afforded the opportunity to initiate computational *in silico* studies that explored possible druggable ExoU sites. Previous work identified a novel drug specific against ExoU activation Methoctramine (N,N′-bis(6-aminohexyl)octane-1,8-diamine), a widely studied muscarinic receptor antagonist [13]. In an initial inhibitor screen, methoctramine was shown to inhibit ExoU activity by 82% (data not shown) [13–17]. The next phase of this work involves repurposing and optimizing the methoctramine scaffold to design a potent ExoU antagonist.

2. Materials and methods

2.1. Protein expression and purification

P. aeruginosa ExoU WT containing gene in a pET15b plasmid was expressed in *Escherichia coli (E. coli)* BL21(DE3)plysS as previously described [11]. In brief, cells were grown at 37°C and ExoU expression was induced when cells reached OD_{600} = 0.8–1.0 with 0.25 mM ispropyl-1-thiogalactopyranoside (IPTG) at 30°C for 3 h. Cells were centrifuged and pellets were stored at -80°C. Pellets were resuspended in 20 mL binding buffer A (5 mM imidazole, 300 mM NaCl, 50 mM Na_2HPO_4, pH 7.0) and 100 μL of protease inhibitor. Sonication was used to lyse cells (15/45 s on/off) for 3 min on ice; the suspension was separated via centrifugation at 20,000 rpm for 20 min at 4°C.

Abbreviations: P. aeruginosa, *Pseudomonas aeruginosa*; *E. coli*, *Escherichia coli*; NMR, Nuclear Magnetic Resonance; STD, Saturation Transfer Difference; MES, Molecular Electrostatic Potential; DPFGSE, Double Pulsed Field Gradient Spin Echo.

* Corresponding author.
E-mail address: tzvia.springer@cuw.edu (T.I. Springer).

https://doi.org/10.1016/j.bbrep.2021.101188
Received 22 October 2021; Received in revised form 7 December 2021; Accepted 11 December 2021

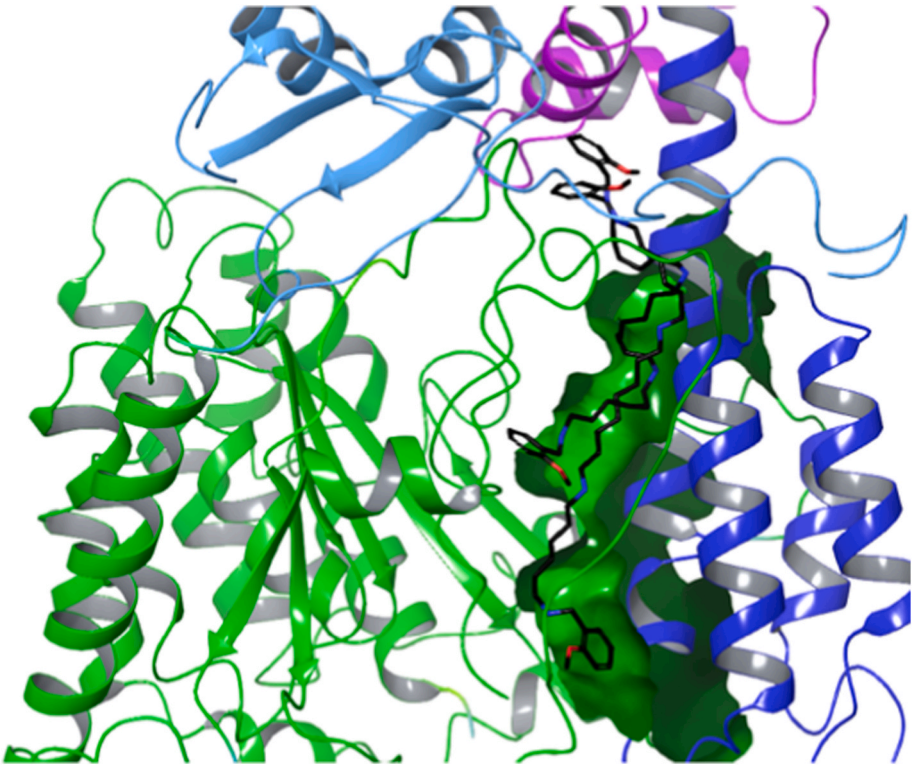

Fig. 1. Cartoon image depicting the functional domains of ExoU; catalytic domain (green), four-helix bundle (dark blue), bridging domain (purple), and ubiquitin binding domain (light blue). Poses of methoctramine (black) predicted to bind a region between the catalytic domain and four-helix bundle. (For interpretation of the references to color in this figure legend, the reader is referred to the Web version of this article.)

Supernatant was passed through a 1 mL HiTrap TALON column and ExoU was eluted with buffer B (500 mM imidazole, 300 mM NaCl, 50 mM Na_2HPO_4, pH 7.0). Validation of protein expression and purification was verified on sodium dodecyl sulfate polyacrylamide gel electrophoresis (SDS-PAGE) stained with Coomassie brilliant blue R-250. Eluted ExoU was concentrated using an Amicon Ultra-15 50-kDa and concentration was determined via a Thermo Scientific NanoDrop 1000 Spectrophotometer. Aliquots of concentrated protein were stored at -80°C in a buffer containing 20% glycerol and 20 mM MOPS, pH 6.8.

2.2. NMR Saturation Transfer Difference (STD)

1D 1H STD-NMR experiments were performed on a Varian 500 MHz spectrometer at 298 K. Samples consisting of ExoU and methoctramine were suspended in buffer (10% glycerol, 10% D_2O, 20 mM MOPS and 150 mM NaCl, pH 6.8). 1D 1H NMR reference spectrum of methoctramine at 250 μM was acquired and a pre-saturation experiment was performed on 5 μM ExoU and 250 μM methoctramine. Using a Watergate suppression experiment, the Double Pulsed Field Gradient Spin Echo (DPFGSE) STD was acquired. FID files were processed and analyzed via SpinWorks_4 4.0 NMR processing software.

2.3. 1D 1H STD-NMR K_D determination

Samples containing increasing concentrations of methoctramine were prepared on ice (100 μM, 125 μM, 150 μM, 175 μM, 200 μM, 225 μM, and 250 μM) in a buffer solution containing 5 μM ExoU. After acquiring a 1D 1H NMR reference spectrum of 300 μM methoctramine, pre-saturation experiments, Watergate suppression experiments and saturation transfer experiments were performed on each sample (n = 3). FID files were processed using SpinWorks_4 4.0 NMR processing software and K_D was determined via a Michaelis-Menten Excel Solver function.

K_D affinity was determined using a Michaelis-Menten Excel Solver and includes equations (1) and (2).

$$\text{STD} - \text{AF} \quad = \frac{\text{Io} - \text{Isat}}{\text{Io}} \text{x} \frac{\text{L}}{\text{P}} \textit{ molar ratio} \tag{1}$$

Equation (1) provides the variation of the STD amplification factor (STD-AF) with increasing concentrations of methoctramine to ExoU. Signal intensities of the reference spectra and saturated spectra, I_o and I_{sat} respectively, provides a comparison of STD effects plotted against methoctramine concentration. STD-AF factors were fitted onto the Michaelis-Menten function equation (2) and were used for Excel Solver predicted values of K_D and $_{\alpha}$STD:

$$\text{STD} - \text{AF} = \frac{\alpha\text{STD}[\text{L}]}{\text{KD} + [\text{L}]} \tag{2}$$

Equation (2) relates STD-AF values to initial velocity (V_0) in the Michaelis-Menten equation, $_{\alpha}$STD portrays the maximum amplification of the reaction (V_{max}) and K_D calculates the concentration of substrate when STD-AF is equal to 1/2 of the $_{\alpha}$STD. K_D and $_{\alpha}$STD factors were determined via solver from Excel.

2.4. Schrödinger Computational Modeling

Protein and ligand preparation, site predictions and initial docking calculations were conducted using Schrödinger Release 2018–3: Schrödinger, LLC, New York, NY, 2021. Each task used default settings unless otherwise mentioned. Protein preparation wizard prepared the protein for site predictions and docking. This included importing the ExoU crystal structure (PDB: 3TU3), assigning bond orders, H-bonds, filled in any missing chains and loops, removed chain A, followed by restrained minimization using OPLS3e force field [18]. Similarly, methoctramine was prepared using Schrödinger's LigPrep tool to generate 3D low energy conformations of the ligand and any possible ionized states at physiological pH [19].

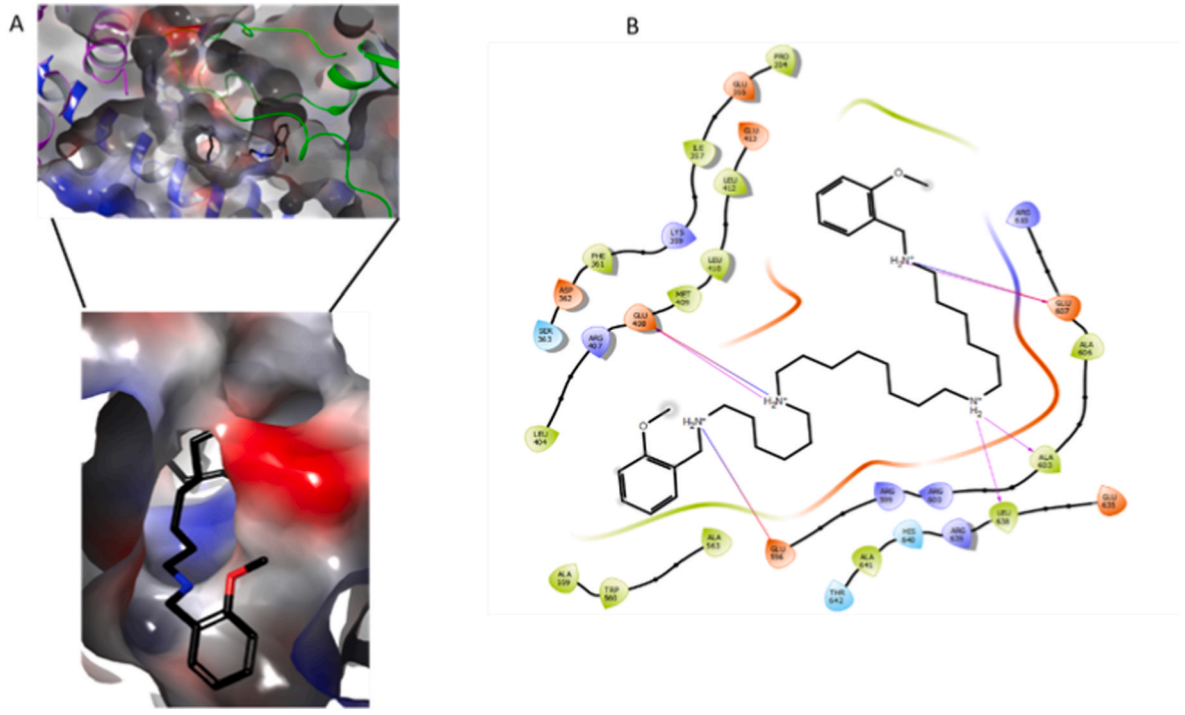

Fig. 2. Methoctramine interaction at the C-terminal domain of ExoU. (A) Methoctramine (black) located in a buried cavity of the C-terminus of ExoU (electrostatic model). (B) Methoctramine ligand interaction diagram within the C-terminal region with a predicted binding score of -11.806 kcal mol^{-1}. Predicted sites of interaction include E607, E408, E596, L638, A603.

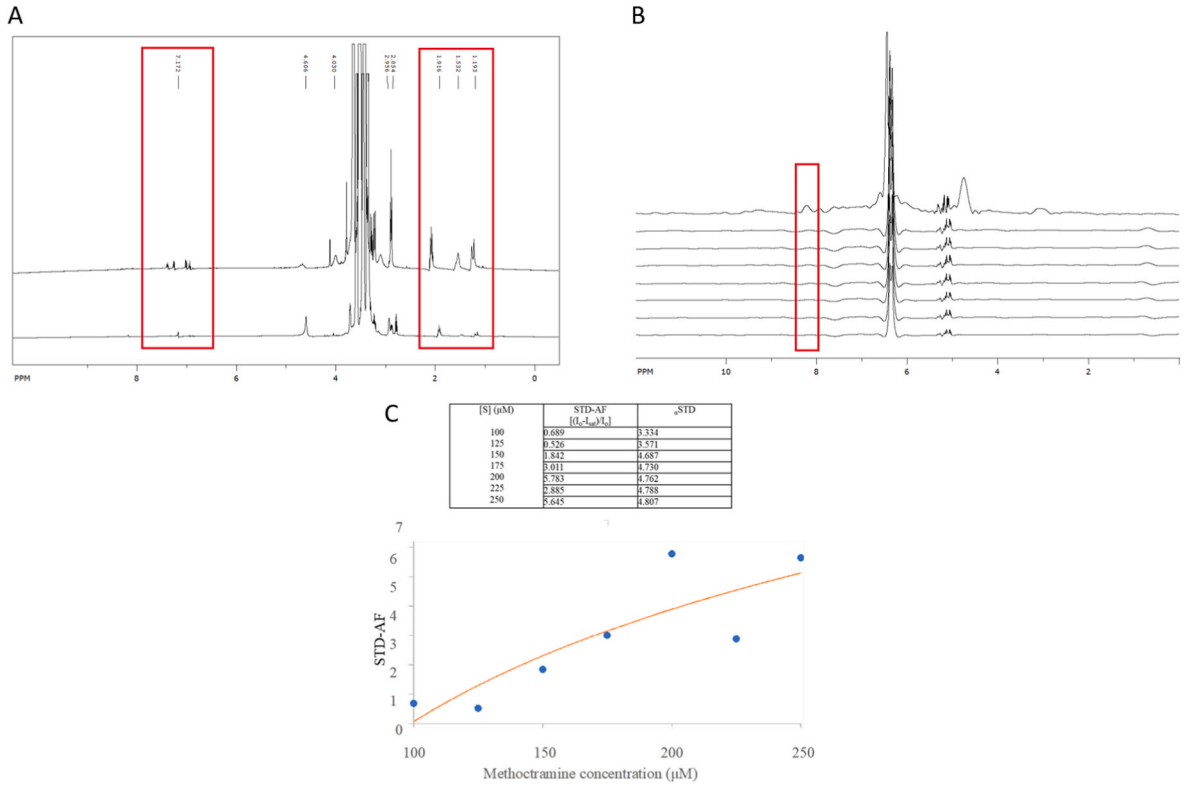

[S] (μM)	STD-AF $[(I_0-I_{sat})/I_0]$	αSTD
100	0.689	3.334
125	0.526	3.571
150	1.842	4.687
175	3.011	4.730
200	5.783	4.762
225	2.885	4.788
250	5.645	4.807

Fig. 3. ExoU and methoctramine 1D STD-NMR (A) 1D STD-NMR spectra at pH 6.8. top: 1D 1H NMR reference spectrum of 250 μM methoctramine, bottom: 1D 1H STD-NMR spectru of 5 μM ExoU and 250 μM methoctramine. Signals relating to aromatic proton (6.9 and 7.2 ppm) and hydrocarbon signals (1.2 and 1.9 ppm) are indicated by the red outlined box. (3B) ExoU and methoctramine K_D 1D 1H STD-NMR titration spectra. Spectra order from top: 1D 1H NMR reference spectrum of 300 μM methoctramine, bottom: 1D 1H STD-NMR spectrum of 5 μM ExoU and increasing methoctramine concentrations (100–250 μM). (3C) STD amplification factors observed (blue) and predicted from equation (1) plotted as a function of methoctramine concentration. STD amplification factors (equation (1)) and estimated K_D and *αSTD* values from equation (2) respective to methoctramine concentration as determined with solver from Excel. (For interpretation of the references to color in this figure legend, the reader is referred to the Web version of this article.)

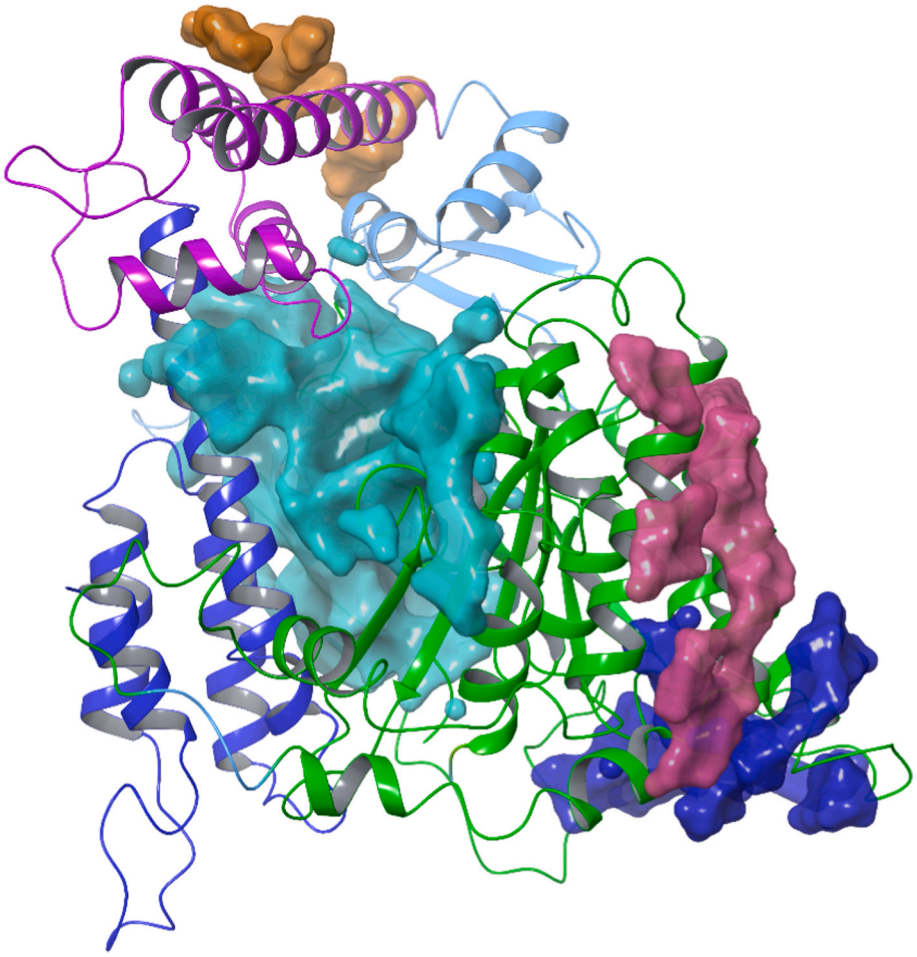

Fig. 4. Druggable sites of ExoU. Top four possible druggable sites of ExoU (ribbon model) represented as surface model colored cyan, magenta, dark blue and orange surfaces respectively. The highest predicted binding affinity site of methoctramine from docking was the cyan region with the highest Dscore of 1.034799 and volume of 3908.142. The Dscore takes into account the size if the site, the degree of enclosure of the site isolated from the solvent and a hydrophilic penalty [20–22]. (For interpretation of the references to color in this figure legend, the reader is referred to the Web version of this article.)

SiteMap [20] was used to explore possible druggable binding sites of ExoU. The prepared methoctramine conformations were then docked, using Glide XP [21] in the top 10 identified sites. SiteMap ranks identified sites using SiteScore and Dscore functions, which both consider size, solvent accessibility, and the hydrophobic/philic nature of the site [20,22]. The ligand with the top ranked docking score that predicts the lowest binding affinity is being considered for further analysis and experimental validation (Fig. 4).

3. Results and discussion

3.1. Schrödinger Computational Modeling

The functional domains of ExoU include the catalytic domain, four helix bundle, bridging domain and ubiquitin binding domains [23] (Fig. 1). Although *in vitro* studies have revealed multiple regions of the protein that may contribute to its cytotoxic quality [12,24,25], there are limited reports, with the exception of phospholipase A2 enzyme inhibitors [26,27], of small molecules that bind those regions resulting in loss of cytotoxicity of ExoU, making drug discovery challenging. We employed the Schrödinger SiteMap tool to identify potential binding sites of methoctramine to ExoU. The top ranked site in which methoctramine was docked aligns and corresponds to the C-terminus region, green surface between the four-helix bundle and catalytic domain (Fig. 1). This region was previously reported to result in diminished cytotoxicity upon multiple amino acid insertions or substitutions within the region (600–687) and would explain the cytotoxicity inhibition exhibited by methoctramine [12,25,28].

Within the buried cavity of the C-terminal domain there are areas that exhibit a variable charge distribution represented by the molecular electrostatic potential (MEP) surface. The red and blue surfaces correspond to electronegative and electropositive regions (Fig. 2). The MEP surface depicts charge and shape complementarity evidenced by a predicted binding score of -11.806 kcal mol^{-1}. The presence of positively charged protonated amines on methoctramine allows for multiple salt bridge and H-bond interactions (E408, E596 and E607) of ExoU C-terminus (Fig. 2B). One amine group makes H-bond interactions with the backbone of L638 and R639, as well as, A603 and V604 (Fig. 2B).

3.2. Validating methoctramine binding to ExoU by NMR spectroscopy

We use NMR spectroscopy to investigate the interaction between ExoU and methoctramine. 1D 1H STD-NMR experiments are resourceful tools for validating potential binding activity between a protein and ligand while identifying the dissociation constant (K_D). In STD-NMR experiments, magnetization is transferred from the macromolecule at a specific irradiation frequency. The transfer of magnetization results in peaks seen from the ligand in the STD-NMR spectrum, indicating a positive result of interaction between methoctramine and ExoU. The STD-NMR experiments resulted in artifacts that display a transfer of magnetization from ExoU to methoctramine, indicative of an interaction between the protein and ligand. When comparing the reference spectrum of methoctramine to the DPFGSE STD spectrum containing both methoctramine and ExoU, aromatic group and hydrocarbon proton signals are observed in both spectra with identical chemical shifts. Aromatic proton signals are observed at 6.9 and 7.2 ppm, whereas the hydrocarbon signals can be seen at 1.2 and 1.9 ppm, suggesting magnetization transfer (Fig. 3A). Intense signals from the buffer solvents

can also be observed due to ExoU buffer requirements (Fig. 3A and B).

The observation of increasing STD-AF factors in correspondence to higher concentrations of methoctramine further suggests an interaction between ExoU and methoctramine. An aromatic signal at 8.3 ppm indicative of methoctramine was highlighted and increasing STD-AF factors of these signals were studied throughout the titration-based experiment (Fig. 3B and C). While noise from excess buffer requirements are seen as intense peaks at ~6.5 ppm, intensities of artifacts indicating ligand alkyl protons can be traced through the stacked spectra for an observable STD effect (Fig. 3B). The predicted $_{\alpha}$STD factors suggest ExoU receptors (specific or nonspecific) to be saturated at concentrations above a ligand:protein ratio of (100 μM:5 μM) due to the decay of αSTD factors in comparison to increasing methoctramine concentrations. The average K_D of methoctramine and ExoU was determined to be 13 ± 1 μM L^{-1} and fits within the range of 10^{-8} mol S^{-1} to 10^{-3} mol S^{-1}, a binding sensitivity threshold recommended for STD experiments.

STD-NMR experiments are one of many robust bioanalytical instrumentation methods for determining potential binding activity, as used in this research for detecting an interaction between ExoU and methoctramine. Successful STD-NMR spectra of 5 μM ExoU and 250 μM methoctramine indicated binding activity between the protein and ligand and supports the hypothesis of methoctramine as a potential precursor to an ExoU small molecule inhibitor. Determination of K_D occurred via a relation of STD-AF signals suggesting binding of ligand protons to an enzyme kinetic relationship of the Michaelis-Menten equation, leading to the prediction of 13 ± 1 μM L^{-1}, a value within the binding affinity sensitivity threshold for such experiments (Fig. 3C). The weak binding affinity from the predicted K_D supports the artifacts seen in (Fig. 3A) suggesting an interaction between methoctramine and ExoU. Future studies to both validate the binding site (Fig. 4) and optimize the structure of methoctramine will include the systematic and rational design of methoctramine analogs from which we can determine structure activity relationship of this structural class. The design of analogs will be guided by structured-based computational modeling. Simultaneously, we will use the methoctramine library of analogs as chemical probes to validate our predicted binding site.Future applications from this research includes *in vitro* hit-to-lead validation of the highlighted novel hit ligand methoctramine in order to investigate binding location and mechanisms for this potential ExoU inhibitor.

Funding

This work was supported by Concordia University Wisconsin (CUW).

Declaration of competing interest

The authors declare no conflict of interest.

Data availability

Data will be made available on request.

Acknowledgements

We acknowledge and thank Dr. Dara Frank and Dr. Jimmy Feix (Medical College of Wisconsin) for the preliminary work and support for this project. We thank Dr. Robert Burlage for manuscript edits.

References

[1] C.R. Hansen, M. Gilljam, H.V. Olesen, N. Hoiby, F. Karpati, E. Johansson, C. Krantz, M. Skov, T. Pressler, A. Lindblad, Maintaining normal lung function in children with cystic fibrosis is possible with aggressive treatment regardless of Pseudomonas aeruginosa infections, Acta Paediatr. 110 (2021) 2607–2609.

[2] K. Kwong, A. Benedetti, Y. Yau, V. Waters, D. Nguyen, Failed eradication therapy of new onset Pseudomonas aeruginosa infections in cystic fibrosis children is associated with bacterial resistance to neutrophil functions, J. Infect. Dis. (2021).

[3] M.D. Parkins, R. Somayaji, V.J. Waters, Epidemiology, biology, and impact of clonal Pseudomonas aeruginosa infections in cystic fibrosis, Clin. Microbiol. Rev. 31 (2018).

[4] H. Sato, J.B. Feix, D.W. Frank, Identification of superoxide dismutase as a cofactor for the pseudomonas type III toxin, ExoU, Biochem. 45 (2006) 10368–10375.

[5] D.M. Anderson, K.M. Schmalzer, H. Sato, M. Casey, S.S. Terhune, A.L. Haas, J. B. Feix, D.W. Frank, Ubiquitin and ubiquitin-modified proteins activate the Pseudomonas aeruginosa T3SS cytotoxin, ExoU, Mol Microbiol. 82 (2011) 1454–1467.

[6] V. Finck-Barbancon, J. Goranson, L. Zhu, T. Sawa, J.P. Wiener-Kronish, S. M. Fleiszig, C. Wu, L. Mende-Mueller, D.W. Frank, ExoU expression by Pseudomonas aeruginosa correlates with acute cytotoxicity and epithelial injury, Mol. Microbiol. 25 (1997) 547–557.

[7] A. Kainuma, K. Momiyama, T. Kimura, K. Akiyama, K. Inoue, Y. Naito, M. Kinoshita, M. Shimizu, H. Kato, N. Shime, N. Fujita, T. Sawa, An outbreak of fluoroquinolone-resistant Pseudomonas aeruginosa ST357 harboring the exoU gene, J. Infect. Chemother. 24 (2018) 615–622.

[8] H.A. Howell, L.K. Logan, A.R. Hauser, Type III secretion of ExoU is critical during early Pseudomonas aeruginosa pneumonia, mBio 4 (2013) e00032-00013.

[9] H. Sato, J.B. Feix, C.J. Hillard, D.W. Frank, Characterization of phospholipase activity of the Pseudomonas aeruginosa type III cytotoxin, ExoU, J. Bacteriol. 187 (2005) 1192–1195.

[10] D.H. Kwon, C.D. Lu, Polyamines increase antibiotic susceptibility in Pseudomonas aeruginosa, Antimicrob. Agents Chemother. 50 (2006) 1623–1627.

[11] T.I. Springer, T.E. Reid, S.L. Gies, J.B. Feix, Interactions of the effector ExoU from Pseudomonas aeruginosa with short-chain phosphatidylinositides provide insights into ExoU targeting to host membranes, J. Biol. Chem. 294 (2019) 19012–19021.

[12] A.S. Halavaty, D. Borek, G.H. Tyson, J.L. Veesenmeyer, L. Shuvalova, G. Minasov, Z. Otwinowski, A.R. Hauser, W.F. Anderson, Structure of the type III secretion effector protein ExoU in complex with its chaperone SpcU, PLoS One 7 (2012), e49388.

[13] J. Jakubik, P. Zimcik, A. Randakova, K. Fuksova, E.E. El-Fakahany, V. Dolezal, Molecular mechanisms of methoctramine binding and selectivity at muscarinic acetylcholine receptors, Mol. Pharmacol. 86 (2014) 180–192.

[14] S. Liu, D. Shi, Z. Sun, Y. He, J. Yang, G. Wang, M2-AChR mediates rapid antidepressant effects of scopolamine through activating the mTORC1-BDNF signaling pathway in the medial prefrontal cortex, Front. Psychiatr. 12 (2021) 601985.

[15] F.V. Lauro, L.R. Maria, L.G. Tomas, D.C. Francisco, G.M. Rolando, R.N. Marcela, M. A. Virginia, G.E. Alejandra, O.A. Yazmin, Design and synthesis of two new steroid derivatives with biological activity on heart failure via the M2-muscarinic receptor activation, Steroids 158 (2020) 108620.

[16] F. Nascimento, L.R.B. Spindler, G.B. Miles, Balanced cholinergic modulation of spinal locomotor circuits via M2 and M3 muscarinic receptors, Sci. Rep. 9 (2019) 14051.

[17] H. Kimura, Y.K. Imura, H. Tomiyasu, T. Mihara, N. Kaji, K. Ohno, T. Unno, Y. Tanahashi, T.R. Jan, H. Tsubone, H. Ozaki, M. Hori, Neural anti-inflammatory action mediated by two types of acetylcholine receptors in the small intestine, Sci. Rep. 9 (2019) 5887.

[18] G.M. Sastry, M. Adzhigirey, T. Day, R. Annabhimoju, W. Sherman, Protein and ligand preparation: parameters, protocols, and influence on virtual screening enrichments, J. Comput. Aided Mol. Des. 27 (2013) 221–234.

[19] S.F. Giardina, D.S. Werner, M. Pingle, P.B. Feinberg, K.W. Foreman, D. E. Bergstrom, L.D. Arnold, F. Barany, Novel, self-assembling dimeric inhibitors of human beta tryptase, J. Med. Chem. 63 (2020) 3004–3027.

[20] T.A. Halgren, Identifying and characterizing binding sites and assessing druggability, J. Chem. Inf. Model. 49 (2009) 377–389.

[21] G. Minuesa, S.K. Albanese, W. Xie, Y. Kazansky, D. Worroll, A. Chow, A. Schurer, S. M. Park, C.Z. Rotsides, J. Taggart, A. Rizzi, L.N. Naden, T. Chou, S. Gourkanti, D. Cappel, M.C. Passarelli, L. Fairchild, C. Adura, J.F. Glickman, J. Schulman, C. Famulare, M. Patel, J.K. Eibl, G.M. Ross, S. Bhattacharya, D.S. Tan, C.S. Leslie, T. Beuming, D.J. Patel, Y. Goldgur, J.D. Chodera, M.G. Kharas, Small-molecule targeting of MUSASHI RNA-binding activity in acute myeloid leukemia, Nat. Commun. 10 (2019) 2691.

[22] T. Halgren, New method for fast and accurate binding-site identification and analysis, Chem. Biol. Drug Des. 69 (2007) 146–148.

[23] M.H. Tessmer, D.M. Anderson, A.M. Pickrum, M.O. Riegert, R. Moretti, J. Meiler, J. B. Feix, D.W. Frank, Identification of a ubiquitin-binding interface using Rosetta and DEER, Proc. Natl. Acad. Sci. U. S. A. 115 (2018) 525–530.

[24] V. Finck-Barbancon, D.W. Frank, Multiple domains are required for the toxic activity of Pseudomonas aeruginosa ExoU, J. Bacteriol. 183 (2001) 4330–4344.

[25] S.D. Rabin, A.R. Hauser, Functional regions of the Pseudomonas aeruginosa cytotoxin ExoU, Infect. Immun. 73 (2005) 573–582.

[26] R.M. Phillips, D.A. Six, E.A. Dennis, P. Ghosh, In vivo phospholipase activity of the Pseudomonas aeruginosa cytotoxin ExoU and protection of mammalian cells with phospholipase A2 inhibitors, J. Biol. Chem. 278 (2003) 41326–41332.

[27] H. Sato, D.W. Frank, C.J. Hillard, J.B. Feix, R.R. Pankhaniya, K. Moriyama, V. Finck-Barbancon, A. Buchaklian, M. Lei, R.M. Long, J. Wiener-Kronish, T. Sawa, The mechanism of action of the Pseudomonas aeruginosa-encoded type III cytotoxin, ExoU, EMBO J. 22 (2003) 2959–2969.

[28] C. Gendrin, C. Contreras-Martel, S. Bouillot, S. Elsen, D. Lemaire, D.A. Skoufias, P. Huber, I. Attree, A. Dessen, Structural basis of cytotoxicity mediated by the type III secretion toxin ExoU from Pseudomonas aeruginosa, PLoS Pathog. 8 (2012), e1002637.